CHEMIJA. 2014. Vol. 25. No. 3. P. 171–184

Electrooxidation of borohydride on a polycrystalline platinum electrode modified with Bi species

Dijana Šimkūnaitė*,

Loreta Tamašauskaitė-Tamašiūnaitė,

Vitalija Jasulaitienė,

Algirdas Selskis

State Research Institute, Center for Physical Sciences and Technology, A. Goštauto St. 9, LT-01108 Vilnius, Lithuania

Surface analysis techniques (XPS and SEM) and electrochemical measurements (cyclic voltammetry) were employed to study borohydride oxidation on a polycrystalline Pt electrode modified with irreversibly adsorbed Bi species in an aqueous alkaline medium containing 0.05 M $NaBH_4$ and 1 M NaOH. X-ray photoelectron spectroscopy revealed the presence of metallic Bi and Bi-oxychloride / hydroxide / oxide on the Pt surface after various immersion times of Pt electrode into a $BiCl_3$ modifying solution in concentrated hydrochloric acid under open-circuit conditions. The Bi-modified polycrystalline Pt electrode exhibited an outstanding electrocatalytic activity for BH_4^- oxidation with hydrogen oxidation highly suppressed implying the inhibition of borohydride hydrolysis reaction. A considerable gain of the current on the Bi-modified polycrystalline Pt electrode can be explained by a gradual conversion of Bi-oxychloride and Bi-hydroxy / oxy surface species into higher valent Bi-oxygenated surface species along with borohydride oxidation. It is supposed that the presence of hydroxylated Bi species on the top of the modifying layer may imply that they act as a donor of hydroxyl species, providing their higher availability on the Bi-modified polycrystalline Pt surface for borohydride oxidation.

Key words: borohydride oxidation, platinum electrode, Bi, cyclic voltammetry

INTRODUCTION

Rapidly rising energy demands require the development and extensive investigation of sustainable power sources alternative to conventional energy supplies. An appropriate choice is the fuel cell noted as an inherently energy efficient, environmentally friendly and silent system. Among various types of fuel cells developed so far, sodium borohydride ($NaBH_4$) has recently emerged as a greatly promising fuel for fuel cells [1–3]. It is known to be converted catalytically to hydrogen and act as hydrogen source [4]

$$BH_4^- + H_2O \rightarrow BH_3OH^- + H_2, \quad (1)$$

as well as to be oxidised and act as an anodic fuel for direct borohydride fuel cells (DBFC) [3, 5, 6]:

$$BH_4^- + 8OH^- \rightarrow BO_2^- + 6H_2O + 8e^-. \quad (2)$$
$$(E^0 = -1.24 \text{ V vs SHE})$$

This dual possibility of borohydrides became a matter of special consideration, especially in the case of DBFC, that has evoked considerable attraction concerning their applications for portable electronic devices [2, 6, 7]. Such cells are of particular interest for a high energy density (9.3 $Wh \cdot g^{-1}$ for

* Corresponding author. E-mail: nemezius@ktl.mii.lt

$NaBH_4$), a high open circuit voltage (1.64 V) and borohydride oxidation reaction (BOR) with theoretically possible complete eight-electrons per borohydride ion (2) [8–10]. However, as a matter of fact, the former reaction (2) is generally followed by spontaneous BH_4^- hydrolysis (1) resulting in hydrogen evolution and BH_3OH^- formation. Both intermediates are supposed to be capable of subsequent oxidation [11–15]:

$$H_2 + 2\ OH^- \rightarrow 2H_2O + 2\ e^-, \quad (3)$$

$$BH_3OH^- + 3\ OH^- \rightarrow BO_2^- + 3/2\ H_2 + 2\ H_2O + 3\ e^- \quad (4)$$

or

$$BH_3OH^- + 6\ OH^- \rightarrow BO_2^- + 5\ H_2 + 2\ H_2O + 6\ e^-. \quad (5)$$

Spontaneous hydrolysis reaction (1) depletes BH_4^- and keeps it from being used in BOR entirely, i.e. two electrons are no longer available to provide electrical energy for every molecule of the hydrogen formed. Therefore this reaction leading to a decrease of faradaic efficiency and reduced power density turns to be the main shortcoming in the performance and practical application of DBFCs.

Regardless of vast investigations, the mechanism and overall oxidation reaction of borohydride remains to be rather complicated and has not been completely disclosed for now [11–13, 16–20]. The number of electrons consumed in BOR markedly depends on the nature of anodic catalyst, solution composition ($[BH_4^-]/[OH^-]$ ratio) and potential applied. A variety of intermediates can be formed at the electrode surface due to the dissociative or molecular adsorption of BH_4^- [20–23]. A set of parallel individual competing oxidation pathways proceeds affecting the rate of overall BOR. Therefore extensive investigations and search for efficient parameters in advancing the application of DBFCs are essential.

The best conditions for complete eight-electron BH_4^- oxidation could be achieved at hydrogen generation highly suppressed. The rate of hydrogen evolution could be significantly decreased by increasing OH^- concentration [24] or by varying the initial concentration of BH_4^- species [11]. On the other hand, the employment of an appropriate anode catalyst demonstrating catalytic inactivity towards borohydride hydrolysis like Au or Ag [14, 15, 17, 25–27] could provide complete eight-electron BH_4^- oxidation. However, the mentioned catalysts perform rather sluggish kinetics. Moreover, Au was shown to be unable to electrooxidise the whole hydrogen formed completely [19, 28–31] and for that reason it cannot be considered as faradaic-efficient BOR electrocatalysts. Much faster kinetics, and therefore better power performance has been observed in the case of Pt, Pd or Ni [19, 32–35]. However, those catalysts are known to be active towards both direct borohydride oxidation and hydrolysis reaction.

Of the vast majority of the catalysts studied [17, 20, 36–41], only few of them showed both a high electrocatalytic activity and a high faradaic efficiency without hydrogen evolution. Such an almost complete direct BOR has been observed in the case of Os/C catalyst [42], presumably Pt [18, 43] and bimetallic PdBi/C and PtBi/C [41]. The addition of thiourea (TU) to borohydride solution suppressed hydrogen evolution by blocking the active sites of the Pt electrode (via adsorption of TU molecule) and showed the transfer of ca. eight electrons, but only at higher potentials [19, 44]. In this sense, the modification of the electrode surface by irreversibly adsorbed species of foreign metals, such as Bi, capable of inhibiting hydrogen evolution [45–50] is expected to change the composition of the catalyst and hence to determine the contribution of individual pathways to the overall BH_4^- oxidation rate. For some metal ions, like Bi^{3+} or Sn^{2+}, irreversible adsorption on the Pt surface occurs spontaneously, i. e., without applying an external current [52–56], and have been previously reported for different systems [49, 51, 57]. However, no data are present on using spontaneously adsorbed Bi species to oxidize borohydride. Besides, most of the investigations focus on metallic nanoparticles or supported metals to affect the appropriate reaction rate, while salts or oxy / hydroxy-species possessing different valency are being screened.

The present paper deals with the physical and electrochemical characterization of a polycrystalline Pt electrode modified with Bi species. The electrocatalytic activity towards borohydride oxidation of the Bi-modified Pt electrode is investigated and is compared with similar characteristics of an unmodified Pt electrode. A combined technique, including surface analysis (scanning electron microscopy (SEM), X-ray photoelectron spectroscopy (XPS)) and electrochemical measurements (cyclic voltammetry (CV)) was employed.

EXPERIMENTAL

Electrochemical measurements were carried out in a conventional three-electrode cell containing 1 M NaOH (Chempur Company) and 0.05 M $NaBH_4$ (Sigma-Aldrich Supply) at 20 ± 1 °C. Analytical grade chemicals and triply distilled water were used to prepare the solutions. Prior to each experiment, the working solution was deaerated with Ar for 0.5 h. The working electrode was a vertical disc of 1 cm^2, made from a polycrystalline Pt foil (99.99% purity, Russia). The counter electrode was a Pt sheet of ca. 4 cm^2 in area. Electrode potentials (E) were measured in reference to the Ag|AgCl|KCl(sat) electrode, unless otherwise stated.

The polycrystalline Pt electrode prior to electrochemical measurements was mechanically polished with diamond pastes down to 0.1 μm, cleaned in sequence in acetone, diluted in HCl and triply distilled water. In order to obtain a clean reproducible surface before each following measurement, the Pt electrode was also scanned in the background 0.5 M H_2SO_4 solution at a potential scan rate (v) of 0.05 $V \cdot s^{-1}$ for 30 min between $E \approx -0.15$ and $E \approx +1.3$ V.

A spontaneous modification of the clean polycrystalline Pt surface was performed in a solution of $BiCl_3$ (ca. 3.5 M),

which was freshly prepared by dissolving $BiCl_3$ in concentrated HCl (both from Alchemy, Czech Republic) to avoid hydrolysis of bismuth chloride. The Pt electrode was spontaneously modified with Bi by immersion of the Pt electrode into the $BiCl_3$/HCl solution under open-circuit conditions at room temperature for 1, 5 and 30 min. Then, its surface was extensively rinsed by triply distilled water and transferred into the electrochemical cell.

For surface structural investigations, the samples were dried in an Ar stream. X-ray photoelectron spectroscopy (XPS) analyses of the modified surface were performed using a spectrometer ESCALAB-MKII VG Scientific (UK) with a source of Mg Co X-ray radiation (300 W) and an Ar^+ ion gun (20 a cm^{-2}). Scanning electrode microscopy (SEM) analyses were performed by using a scanning electron microscope EVO-50 (Carl Zeus, 2005). All electrochemical measurements were recorded using a μAutolab Type III (Eco Chimie).

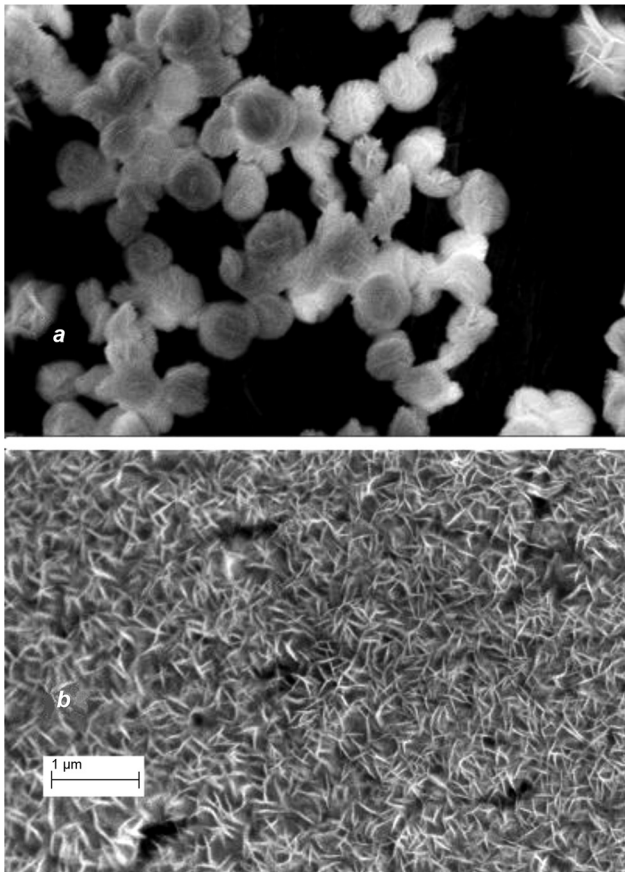

Fig. 1. SEM images of bismuth nanoparticles on the polycrystalline Pt electrode obtained by immersion of the Pt electrode into $BiCl_3$/HCl solution under open-circuit conditions for 1 min (*a*) and 30 min (*b*)

RESULTS AND DISCUSSION

Physical characterization

To provide structural and morphological information of a spontaneously Bi-modified Pt electrode surface SEM and XPS were performed. Figure 1(a, b) shows typical SEM images of bismuth nanoparticles randomly distributed over a polycrystalline Pt surface obtained by immersion of the Pt electrode into $BiCl_3$/HCl solutions under open-circuit conditions for 1 and 30 min. Individual spherical-sized particles above several hundred nm in size forming a large network occur when a short modification time, t_{imm} = 1 min, is applied (Fig. 1a). When the immersion time is increased to t_{imm} = 30 min mostly nanofibre-like structures develop and clearly dominate (Fig. 1b).

The XPS data characterizing the surface state and elemental composition of the spontaneously modified polycrystalline Pt surface with bismuth species obtained by immersion of the Pt electrode into the modifying solution under open-circuit conditions for 1 and 30 min are presented in Table 1. The elemental composition of the modifying layer differs depending on the Pt electrode modification time applied. When the Pt electrode is exposed to the $BiCl_3$/HCl solution for 1 min, the modified surface contains ca. 10.43 at. % of Bi, ca. 61.08 at. % of Pt, ca. 22.82 at. % of oxygen and ca. 5.66 at. % of Cl (anion from modifying solution). A more pronounced increase in Bi to ca. 23.05 at. %, oxygen to ca. 32.7 at. %, Cl to ca. 28.64 at. % and a significant decrease of in Pt to ca. 16 at. % are observed after 30 min. immersion. The overall elemental composition indicates the discontinuous modifying layer or even submonolayer coverage of modifying species developed after modification of the electrode surface (Table 1).

A more detailed analysis of the XP spectra characterizing the surface state and elemental composition of the modified polycrystalline Pt surface with bismuth species after 30 min immersion is presented in Table 2 and Fig. 2. The data on the surface elemental composition clearly show the presence of irreversibly adsorbed Bi species (both metallic and oxidized) on Pt. Ar^+ sputtering for 15 s (i. e. down to a 1 nm sputter depth) gradually removes the modifying layer and results in a slight decrease in Bi to ca. 22.97 at. %, oxygen to ca. 20.45 at. %, Cl to ca. 15.02 at. % and provides an increase in Pt amount to ca. 41.56 at. %. While upon 30 s Ar^+ sputtering (what corresponds to a 2 nm sputter depth) a quite negligible decrease in Bi to ca. 22.87 at. % was observed. Corresponding values for O and Cl decrease to ca. 17.9 and 3.6 at. %, respectively.

The XP spectra of Bi 4f, Cl 2p, O 1s and Pt 4f when Ar^+ sputtering was not applied and upon Ar^+ sputtering for 30 s

Table 1. **XPS data of the elemental composition of the modifying layer after spontaneous modification of the polycrystalline Pt surface by bismuth species at open circuit conditions for different immersion times**

Immersion time, min	Pt, at. %	Bi, at. %	O, at. %	Cl, at. %
1	61.08	10.43	22.82	5.66
30	15.61	23.05	32.7	28.64

are presented in Fig. 2a–h. Typical Bi 4f spectra display a doublet consisting of a low energy band (Bi $4f_{7/2}$) and a high energy band (Bi $4f_{5/2}$) (Fig. 2a). To identify different oxidation states of Bi for the case when Ar^+ ions sputtering was not applied, the Bi $4f_{7/2}$ spectrum was deconvoluted into three peaks centered at 157.78 eV, 159.48 eV and 160.1 eV (Table 1, Fig. 2a). It is necessary to point out some features inherent to XP spectra interpretation. The main trouble is that we cannot exclude the oxidation by air during sample transfer and therefore the XP spectra can be influenced at least partially by oxygen. So, it is hardly possible to propose an unambiguous treatment of the results obtained in the case when Ar^+ sputtering was not applied. However, the values obtained point to the fact that the surface layer can initially be comprised of metallic Bi, bismuth oxide/hydroxide and bismuth oxychloride.

Typically the binding energies of $4f_{7/2}$ level for the metallic Bi range from 156.6 to 157.1 eV [58]. The one determined by us at 157.8 eV is close to that found for the Bi-modified Pt(111) surface (i. e. 157.6 ± 0.1 eV) [59] or polycrystalline Pt (i. e. 157.4 eV) [60] and similarly can be assigned to Bi(0). The shift in BE towards higher values of about 0.5 eV [59] was explained by a rather strong Bi-Pt bond, resulting in a positive charge on the Bi atom, followed by the influence of coadsorbed anions contributing to the shift in Bi spectral lines. An analogous shift to higher BE values for polycrystalline Pt modified with bismuth species as compared with

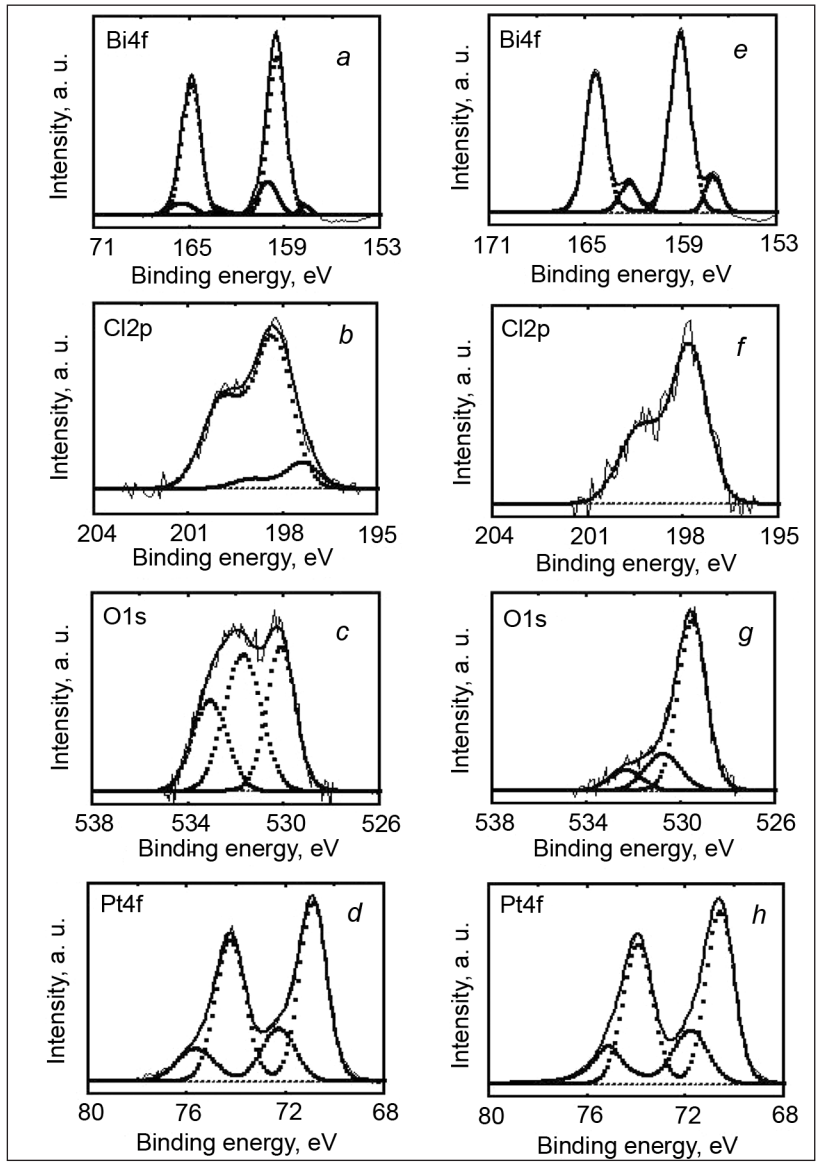

Fig. 2. Representative XP spectra of the Bi-modified polycrystalline Pt surface, when Ar^+ was not applied (*a–d*) and after 30 s (*e–h*) Ar^+ sputtering (i. e. 2 nm sputter depth) for binding energies of bismuth 4f (*a, e*), chlorine 2p (*b, f*), oxygen 1s (*e, g*) and platinum 4f (*d–h*). The polycrystalline Pt electrode was modified by immersion of the Pt electrode into $BiCl_3$/HCl solution under open-circuit conditions for 30 min

Table 2. **XPS analysis of the elemental composition of the modifying layer after 30 min modification of the polycrystalline Pt surface by bismuth species at open circuit conditions and the corresponding composition depending on the Ar^+ sputtering time applied**

Ar^+ sputter time, s	Element	Composition, at. %	Level	Binding energy, eV
0	Pt	15.61	Pt $4f_{7/2}$	70.89 and 72.3
	Bi	23.05	Bi $4f_{7/2}$	157.78, 159.48 and 160.1
	O	32.7	O 1s	530.14, 531.74 and 533.1
	Cl	28.64	Cl 2p	197.41 and 198.35
15	Pt	41.56	Pt $4f_{7/2}$	70.79 and 72.1
	Bi	22.97	Bi $4f_{7/2}$	157.43 and 159.46
	O	20.45	O 1s	530.02, 531.54 and 533.0
	Cl	15.02	Cl 2p	198.13
30	Pt	55.62	Pt $4f_{7/2}$	70.6 and 71.81
	Bi	22.87	Bi $4f_{7/2}$	156.99 and 159.06
	O	17.9	O 1s	529.54, 530.77 and 532.36
	Cl	3.6	Cl 2p	197.8

those obtained for massive bismuth metal samples [60] was realized as a consequence of an electronic charge transfer to the metal.

Another BE value at 159.48 eV can obviously arise due to adsorbed oxidized Bi^{3+} species, i.e. Bi_2O_3 with hydroxylated ones as BiO(OH) [58–61]. The highest BE at 160.1 eV could be attributed to bismuth oxychloride [58, 62, 63]. The latter supposition can be supported by the XP spectra of Cl 2p being constituted of two components with BE at 197.41 and 198.35 eV (Fig. 2 b). They could be related to chloride anions and bismuth oxychloride, respectively.

Upon Ar^+ sputtering for 30 s the lowest BE value shifts from 157.8 to 156.99 eV (minor component) (Fig. 2e) and coincides with that for true metallic Bi. Meanwhile, bismuth oxide / hydroxide and bismuth oxychloride BE values at 159.48 eV and at 160.1 eV contribute to one BE peak at 159.09 eV that appears to be dominant as compared to the lower BE peak at 156.99 eV for true metallic Bi, regardless of the increased fraction of the minor component at 156.99 eV (Fig. 2e). Simultaneously, the XP spectra of Cl 2p turn into one peak centered at 197.8 eV upon 30 s Ar^+ sputtering, indicating the descending contribution of Bi-oxychloride (Table 2, Fig. 2f). Such an alteration in BE's upon Ar^+ sputtering denotes changes in the fractions of the chemical states of bismuth and tentatively points to the increasing availability of Bi_2O_3 underneath BiO(OH) and bismuth oxychloride species in the modifying layer in the presence of irreversibly adsorbed metallic Bi. This assumption is in agreement with the proposed model [61], where the PtBi alloy was supposed to be covered by a layer of Bi_2O_3 with BiO(OH) species on the very top of the layer. Moreover, this suggestion is in line with the explanation [60], where the Bi layer was supposed to consist of multilayer islands with the very first Bi upd layer attached to Pt and air-oxidized or specifically adsorbed Bi species confined to the electrode.

The availability of BiO(OH) and bismuth oxychloride species mainly on the top of the modifying layer additionally could be also supported by the analysis of binding energies for the O1s spectral lines. The XP spectra of O 1s before Ar^+ sputtering (Fig. 2c) split into three resolved peaks centered at 533.1, 531.74 and 530.14 eV turning into 532.36, 530.77 and 529.54 eV with the lowest becoming dominant upon 30 s Ar^+ sputtering (Fig. 2g). The highest BE value at 533.1 eV converting into 532.36 eV is generally related to physically adsorbed water molecules [60, 64]. The lowest energy contributions at 530.14 and 529.54 eV (i.e. before and after Ar^+ sputtering, respectively) can be assigned to oxide species like Bi_2O_3 and PtO ([58–60, 64, 65]). Correspondingly, the last BE value at 531.74 eV can be attributed to bismuth oxychloride / hydroxide. It transforms into a lower intensity BE peak at 530.77 eV upon 30 s Ar^+ sputtering. BE ranging from 531 to 531.5 eV and even to 531.9 eV are typical of OH^- species [59, 60].

The transformation of the XP spectra of Cl 2p into one BE peak (Fig. 2b, f) and other aforesaid factors offer a relative decrease in bismuth oxychloride species upon sputtering making BE components undetectable, supposing that bismuth oxychloride species should be ruled out deep inside the modifying layer. So, the interpretation of the O 1s spectra in relation to Bi 4f and Cl 2p confirms the presence of bismuth oxychloride / (hydr)oxide in the modifying layer and points to the gradual removal of bismuth oxychloride / hydroxide upon sputtering with occurrence of the clearly dominating lowest BE peak at 529.54 eV for oxide species.

Subsequently, the Pt 4f spectra give a doublet of a high energy band (Pt $4f_{5/2}$) and low energy band (Pt $4f_{7/2}$) (Fig. 2d). Deconvolution of the latter reveals two peaks centered at 70.89 and 72.3 eV. Upon 30 s Ar^+ sputtering they slightly shift to the lower BE values at 70.6 and 71.81 eV (Fig. 2h). The presence of the two peaks indicates that Pt was in two different oxidation states, Pt(0) and Pt(II). However, the lower BE peak clearly dominates and can be attributed to metallic Pt, while the higher BE peak can be related to PtO, respectively (Fig. 2d, h). The Pt 4f XP spectra denote the presence of a discontinuous modifying layer, developed after modification of the electrode.

Overall XPS data confirm the presence of both metallic bismuth and its oxy-species on the Pt surface after spontaneous modification under open-circuit conditions with the bismuth oxychloride / hydroxide predominantly located at the very top of the modifying layer.

Electrochemical characterization

Cyclic voltammograms of bare and Bi-modified Pt electrodes in a 1 M NaOH solution for different modification times when the electrode potential is scanned to progressively more positive values are presented in Fig. 3. The CV curves of the bare Pt electrode can be characterized by three potential regions as follows: (a) a hydrogen adsorption / desorption region ($-0.9 < E < -0.6$ V), (b) a double layer region ($-0.6 < E < -0.45$ V), and (c) a hydroxide-oxide formation region ($-0.45 < E < 0.6$ V). Two kinds of oxygen containing species like PtOH and PtO can be generated regarding the potential region applied [66]. Commonly the potential domain up to c. a. –0.10 V is related to OH^- ion electrosorption with charge transfer and formation of surface hydroxides ($OH^- \rightarrow OH_{ad} + e^-$ in alkaline solutions) [67–69]. Their adsorption on Pt in an alkaline medium starts quite early, as soon as desorption of H ceases [70, 71]. Reversible and weak OH_{ad} adsorption inherent to the mentioned potential domain is followed by another one where irreversible, more stable, strong bounded OH_{ad} species along with the higher valent oxides are formed. Typically, the most positive potential region raging up to 0.6 V is associated with stoichiometrically different Pt-OH species, that transform into Pt-O^-, Pt = O or Pt_2 = O depending on the surface coverage of strongly adsorbed OH_{ad} and is catalyzed by OH^- [72, 66]. Besides, the surface coverage of strongly adsorbed OH_{ad} is known to increase when successive cycling is applied [72]. Such aforementioned oxidation regions have been observed for both Pt(111) [66, 68, 69] and

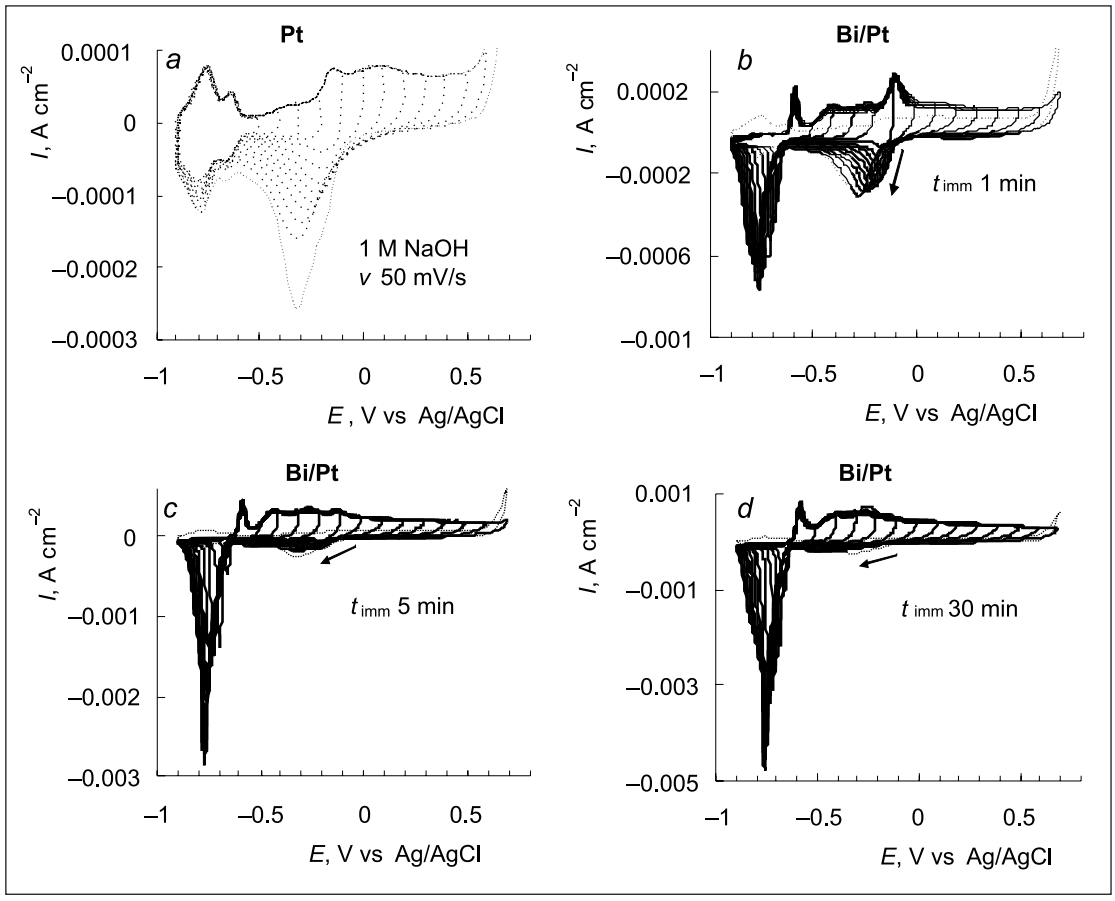

Fig. 3. Cyclic voltammograms for the bare polycrystalline Pt electrode (*a*, dotted lines) and the Bi-modified polycrystalline Pt electrode (*b–d* full lines) in 1 M NaOH solution obtained by immersion of the Pt electrode into a $BiCl_3$/HCl solution under open-circuit conditions for 0 (*a*), 1 (*b*), 5 (*c*) and 30 (*d*) min with a progressive increase (increment of 0.1 V) in the upper potential limit from –0.9 to 0.7 V. Potential scan rate $v = 50$ mV s^{-1}

polycrystalline Pt [72] electrodes and appeared to be close to those determined by us.

General cyclic voltammograms shapes of the Bi-modified Pt electrode at different modification times for scanning electrode potential by gradual increasing the upper potential limit up to 0.7 V reveals that an increase in Pt electrode immersion time into the modifying solution results in the higher anodic current densities (Fig. 3b–d). However, hydrogen adsorption / desorption features, typical of clean polycrystalline Pt in an alkaline solution, are largely suppressed on Bi-modified Pt electrodes in the potential region from –0.9 to –0.65 V for all the immersion times applied. This clearly confirms the presence of blocking species on the Pt surface. More detailed plots of scanning electrode potential to progressively more positive values up to the 0.0 V potential limit are shown in Fig. 4. In all cases a pronounced anodic current peak centered at ca. –0.6 V in the positive-going sweep is observed. It arises in a double layer region, where the faradaic process of weak OH^- ions adsorption takes place with very low coverages and, consequently, negligible charges [67, 73]. Switching potential at –0.5 V an equally expressed narrow cathodic peak at ca. –0.68 V emerges. Successive cycling within this potential region does not influence the shape of CV curves, keeping them superimposed (Fig. 4 insets). The calculated charges from positive and negative current peaks for 1, 5 and 30 min immersion of the Pt electrode into the modifying solution are 0.22 and –0.30 mC, 0.41 and 0.41 mC, 0.87 and 0.88 mC, respectively. This points to the presence of relatively stable bismuth-modifying species on the surface and suggests the formation of a redox couple of Bi-oxy-species on Pt. The redox peaks observed are in line with the previously reported ones for irreversibly adsorbed Bi on the Pt(111) electrode in the presence of chloride [74], or on polycrystalline Pt [75, 57], and are similar to those for a bulk PtBi alloy [61] in acidic solutions. It should be noted that the above mentioned couple is entirely absent in solutions of perchloric acid as was stated by Bowells [74] and not observed for the Bi-modified Pt(111) electrode [56, 76]. In accordance with the XPS data (see Fig. 2 a, b, e, f) this redox couple could be attributed to the adsorbed Bi-oxychloride.

The increase in the upper potential limit up to –0.1 V makes no influence on the anodic current peak centered at –0.6 V, whereas new poorly pronounced anodic peaks have developed in the potential region from ca. –0.5 V to –0.2 V (Fig. 4a, b, c). They are followed by a well-defined peak at –0.1 V in the case of 1 min electrode modification time,

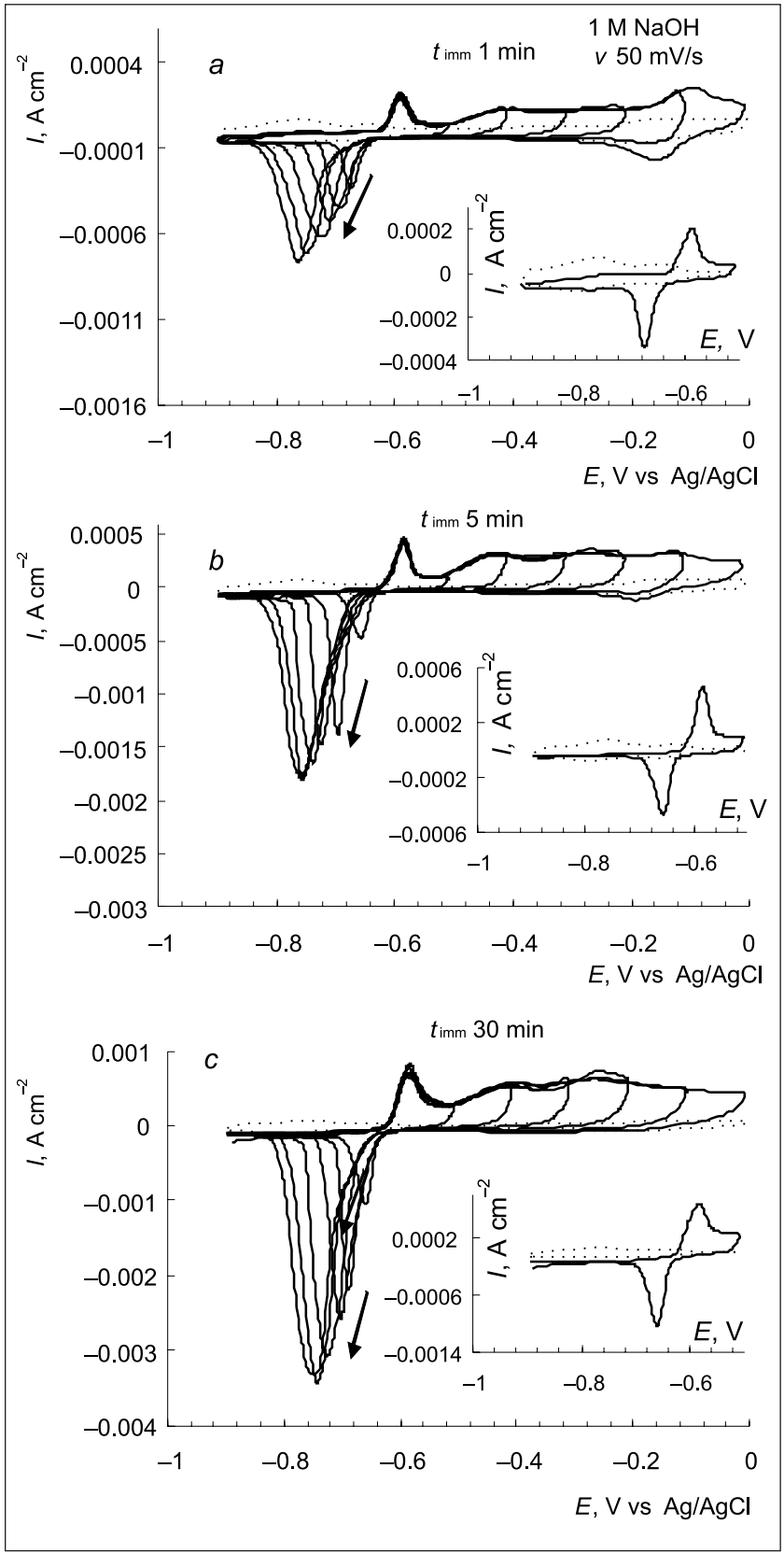

Fig. 4. Cyclic voltammograms for the bare polycrystalline Pt electrode (dotted lines) and Bi-modified polycrystalline Pt electrode (full lines) in 1 M NaOH solution obtained by immersion of the Pt electrode into $BiCl_3$/HCl solution under open-circuit conditions for 1 (*a*), 5 (*b*) and 30 (*c*) min with a progressive increase (increment of 0.1 V) in the upper potential limit from –0.4 to 0.0 V. Potential scan rate $v = 50$ mV s^{-1}. Insets represent cyclic voltammograms at multifold cycling in the potential domain from –0.9 to –0.5 V for the each immersion time applied

meanwhile, for other modification times this peak is less expressed and is substantially screened. The mentioned current features for different modification times scanning electrode potential from –0.9 to 0.7 V are quite apparent in Fig. 5. It should be noted that in the former potential domain, i. e. at $E = -0.45$ V the presence of Bi_{upd} with an adsorbed mixed oxide-hydroxide layer on the top of the latter for the Bi-modified Pt electrode in a NaOH solution on the basis of XP spectra analysis was confirmed [60]. Moreover, on the ground of the potential-pH diagram of bismuth [77], within the potential ranges of our experiment in a 1 M NaOH solution (pH 14), the following redox reactions can take place:

$$2Bi_2O_3 + 2OH^- = Bi_4O_7 + H_2O + 2e^-$$
$$E_0^1 = 1.338 - 0.059\ pH, \quad (6)$$

$$Bi_4O_7 + 2OH^- = 2Bi_2O_4 + H_2O + 2e^-$$
$$E_0^2 = 1.544 - 0.059\ pH, \quad (7)$$

$$Bi_2O_4 + 2OH^- = Bi_2O_5 + H_2O + 2e^-$$
$$E_0^3 = 1.607 - 0.059\ pH. \quad (8)$$

The potential values with regard to pH for each reaction are close to 0.512, 0.718 and 0.781 V (vs RHE) (which corresponds to –0.515, –0.309 and –0.246 V vs Ag/AgCl), respectively. All these species, involved in the reactions, are known to be stable in an alkaline medium [77]. Consequently, poorly pronounced multi-peaks could be related to gradual conversion of Bi-oxychloride to higher valent Bi-hydroxy / oxy surface species. Regardless of a very few references on the Bi/Pt electrode in the alkaline media, the final anodic peak located at ca. –0.1 V is in good agreement with the previous findings for Bi modified polycrystalline Pt by Kadirgan et al. [78] or by Schmidt et al. for Pt(111) [76]. Generally, the surface process associated with this peak for the Bi modified Pt electrode is attributed to the enhanced formation of OH_{ad} / oxygenated species on the Pt sites adjacent to Bi adatoms due to lowering of the local potential of zero charge (pzc) [76]. The enhanced forma-

tion of the surface oxide layers at more positive potentials was also denoted [76, 79].

The corresponding negative-going scans with a gradual reversal of the anodic potential limit up to –0.1 V are described by hardly discernable cathodic current features due to the overlap of the peaks in the double layer region (Fig. 3b). They are followed by a distinct increase in cathodic current in the hydrogen adsorption region with the peak shift in the negative potential direction. The latter starts to decrease after the anodic potential switching at 0.0 V and splits into some separate peaks with the further opening potential window up to 0.7 V (Figs. 3, 5). Simultaneously, a negligible decrease in the anodic current peak at ca. –0.6 V for the positive going scan is observed. Analogous cathodic peak splitting was observed in the case of PtBi alloy [61]. Development of the few peaks after more aggressive electrochemical pretreatment could be similarly assigned to the reduction of surface Bi oxygenated species [61] since the upper potential limit lies in the region where more stable and strong bounded OH_{ad} species along with oxide layer formation are available. Meanwhile, the cathodic peak located around –0.2 V is characterised by the increasing irreversibility of the process and is in line with general behaviour of oxide layers reduction on Pt [72, 80] (Fig. 3). The irreversibility is interpreted by the increasing role of strong bounded OH_{ad} and of higher valent oxides that are stabilized by coadsobed Bi adatoms that incorporate in the surface oxides at high potentials [79]. However, the cathodic current on the Bi-modified polycrystalline Pt electrode for 1 min electrode modification time is higher than that achieved for 5 or 30 min modification time and is higher when compared to the current for the unmodified Pt electrode with a potential peak location at more positive potential (Fig. 5). It can be explained by the presence of more easily oxidisable species on the surface protecting Pt from oxidation [81]. Following the potential-pH diagram of bismuth species [77] the Bi-modified Pt electrode surface is under Bi_2O_5 form in the high potential domain. It undergoes reduction into Bi_2O_4 by Eq. (8) in the potential region where oxygen reduction proceeds. The reduction of these higher valence Bi oxyspecies leads to the development of Bi oxygenated species-free Pt sites that become available for oxygen reduction and explains the shift of the reduction wave towards higher potential. Meanwhile the bismuth-rich surface results in a higher coverage of Pt by Bi species leading to a lower number of active sites for oxygen adsorption and therefore a lower reaction rate with the shift of the reduction wave towards the lower potential region.

It should be noted that underpotential deposition of Bi in an alkaline solution was shown to take place in between –0.3 and –1.2 V vs MSE [82], which corresponds to our conditions to 0.15 and –0.75 V vs AgCl. Furthermore, the presence of small amounts of adsorbed OH_{ad} species on the Pt(hkl) surface in alkaline solutions was proved in the hydrogen underpotential deposition (H_{upd}) region [68, 73]. The coupled competing adsorption / desorption process of H_{upd} and OH_{ad} therein occurs [76]. The coexistance of OH_{ad} in the H_{upd} potential region implies that the potential-dependent surface coverages by H_{upd} and OH_{ad} in alkaline solutions cannot be obtained by simple coulonometry [73] and, moreover, the coverage of the residual Bi-adlayer cannot be quantified from the H-upd charge due to the overlap of the redox peaks related to Bi-oxy-species and the H-upd features [76].

Borohydride oxidation

Figure 6 shows sodium borohydride oxidation on the unmodified and on Bi-modified Pt electrodes in a 1 M NaOH solution at 0.05 V s^{-1}. The first scans for different electrode modification times applied are presented in the inset in Fig. 6a. A pronounced anodic current peak at low potentials on the first scan over the bare polycrystalline Pt electrode arises (Fig. 6a). It reduces appreciably with further cycling. Practically reproducible voltammograms appear in a few successive cycles. The obtained voltammetric data for the polycrystalline Pt electrode, as well as these reported in [18,

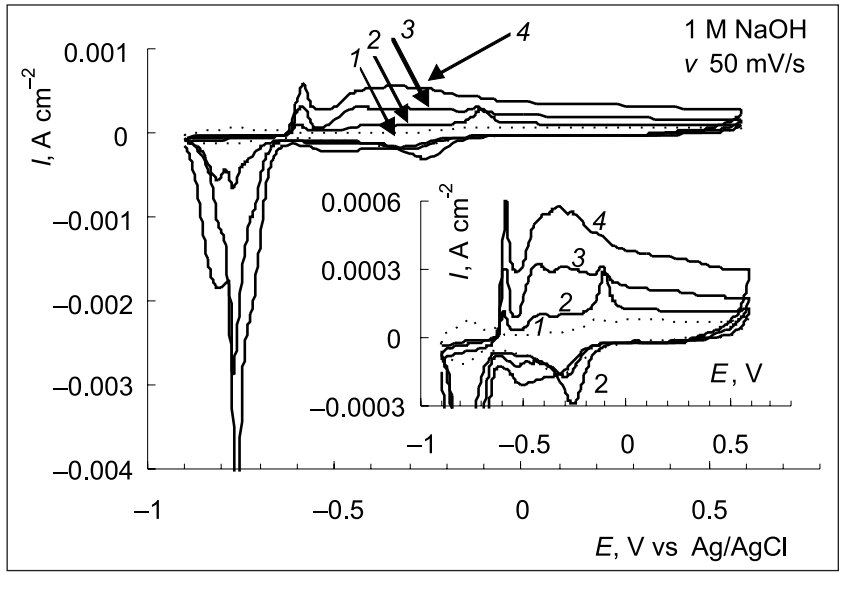

Fig. 5. Cyclic voltammograms for the bare polycrystalline Pt electrode (dotted lines) and Bi-modified polycrystalline Pt electrode (full lines) in 1 M NaOH solution obtained by immersion of the Pt electrode into $BiCl_3$/HCl solution under open-circuit conditions for different t_{imm}, min: *1* – 0, *2* – 1, *3* – 5, *4* – 30. The inset denotes cyclic voltammograms at an increased scale

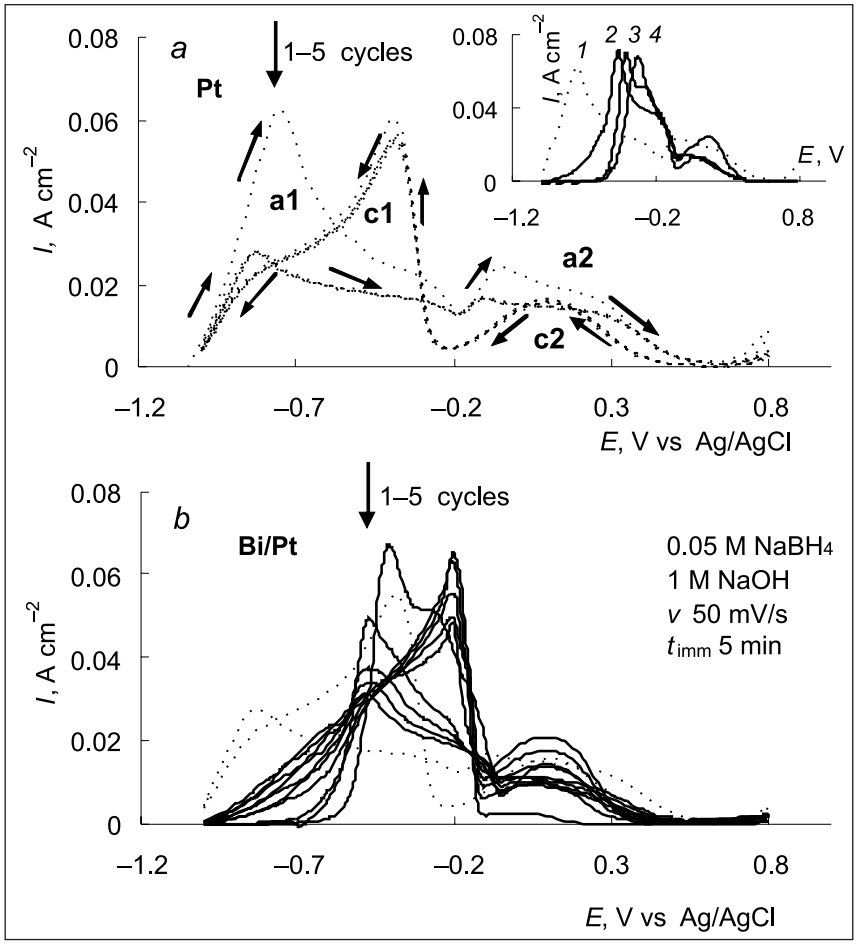

Fig. 6. Cyclic voltammograms for the unmodified polycrystalline Pt electrode (*a*) and for 5 min Bi-modified polycrystalline Pt electrode (*b*) in 1 M NaOH + 0.05 M $NaBH_4$ solution, at the potential scan rate $v = 50$ mV s^{-1}. The dotted line (*b*) represents the stabilised cyclic voltammogram curve over the unmodified polycrystalline Pt electrode. The inset shows the first scans of cyclic voltammogram curves obtained by immersion of the polycrystalline Pt electrode into $BiCl_3$/HCl solution under open-circuit conditions for different t_{imm}, min: *1* – 0, *2* – 1, *3* – 5, *4* – 30

26, 72] show that the voltammograms do not undergo radical transformations and are similar in shape. CV curves are typically associated with four characteristic oxidation peaks; i. e., two on the positive-going sweep and another two on the negative-going sweep labelled as a1, a2, c1 and c2, respectively. They are defined by the waves broadly lying in the potential regions between –1 and –0.3 V and between –0.15 and 0.8 V on the anodic scan, followed by another two between 0.8 and –0.15 V and between –0.2 and –1 V on the cathodic scan.

At low potentials the current is supposed to increase due to BH_4^- oxidation, resulting in peak a1, where the process is complicated by spontaneous hydrolysis reaction (1) since the BH_4^- open circuit potential is at more negative value than the H_2 potential on Pt [11, 16]. Meanwhile, the oxidation potential of intermediate BH_3OH^- is considered to be more negative than that of BH_4^- [9, 15, 28]. Therefore, borohydride oxidation is followed by the reactions (3–5) in a broadly lying potential domain of wave a1 up to –0.3 V. Regardless that BH_4^- electrooxidation on the Pt surface has been a relatively active research subject, there is no consensus in the interpretation of the processes occurring in the first oxidation wave a1 up to date. Recent electrochemical studies suggest that the electrooxidation of BH_4^- on Pt at low potentials proceeds via a direct pathway [18, 34], an indirect pathway [26, 72, 83] and by a partial borohydride hydrolysis or a direct borohydride oxidation reaction [20]. However, the above mentioned wide potential domain of CV curves coincides with the response for the positive-going potential scan in the supporting electrolyte where weak and reversible OH_{ad} electrosorption occurs (Fig. 3a). Reasonably, an oxygen source for borohydride oxidation is here assumed to be OH^- ions from a solution by the Eley-Rideal-type mechanism [26, 72].

The second anodic oxidation wave a2 at higher potentials, located between –0.15 and 0.8 V (Fig. 6), is commonly attributed to the direct BH_4^- oxidation pathway with 5 or 6 e^- involved [26, 72] and is associated with electrosorbtion of OH^- and formation of OH_{ad} on Pt [18, 20, 26, 72]. BH_4^- oxidation in the potential domain of wave a2 is less efficient than that on bare platinum, since it proceeds on a partially oxidised Pt surface with the irreversibly adsorbed OH_{ad} or Pt oxides formed.

On the reverse cathodic going potential sweep two oxidation waves c2 and c1 at ca. +0.3 and –0.3 V, respectively, are considered to have a "cleaning" effect on the electrode surface, however, their interpretation also faces some differences [18, 72].

The presence of bismuth species on the Pt electrode shows substantial differences in the polarization curves (Fig. 6b). Wave a1 at low potentials is largely inhibited on the Bi-modified polycrystalline Pt electrode. It starts at more positive potentials than on the bare Pt electrode, provides higher current densities and depends on the potential scans

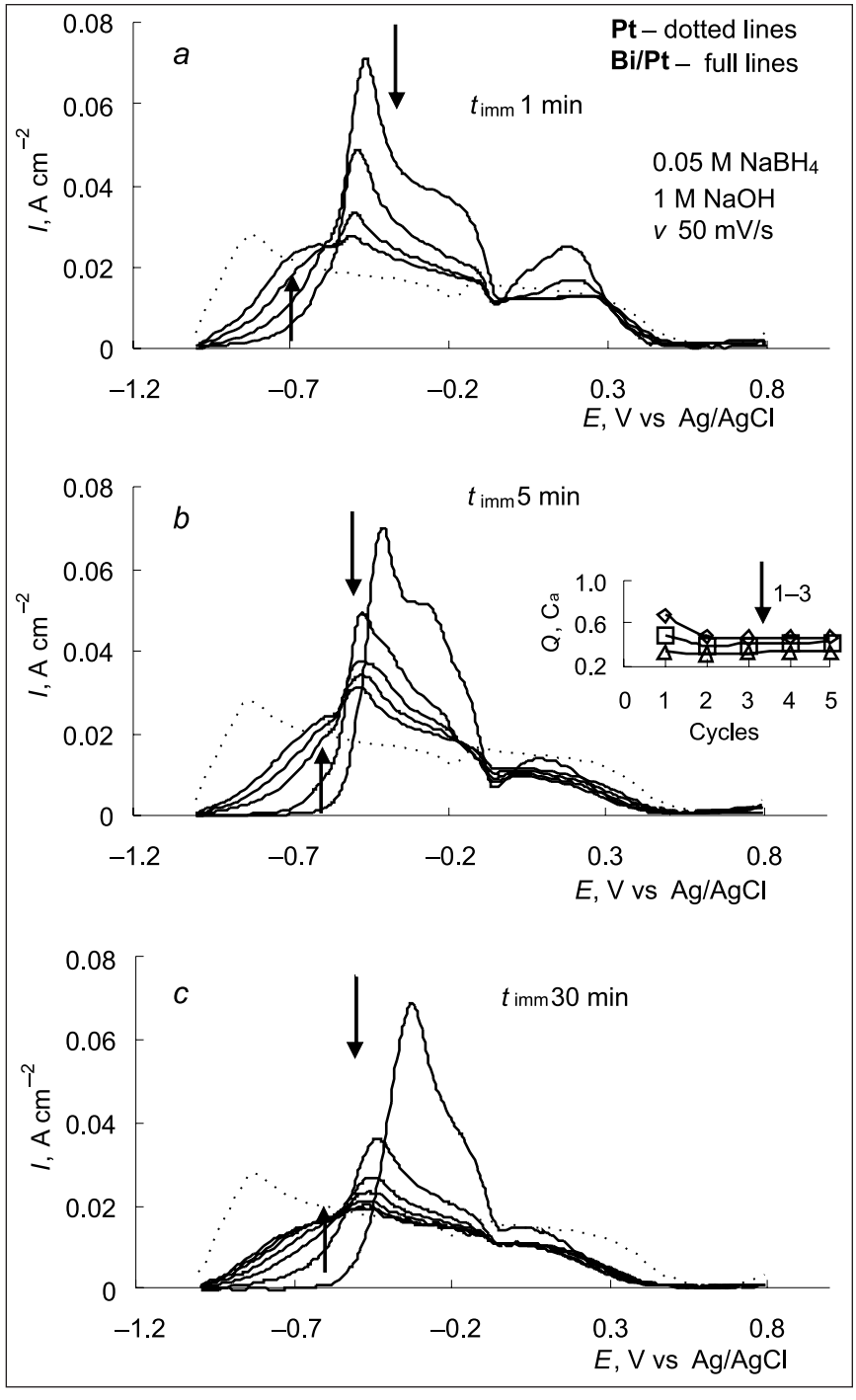

Fig. 7. Cyclic voltammograms for the bare polycrystalline Pt electrode (dotted lines) and the Bi-modified polycrystalline Pt electrode (full lines) in 1 M NaOH + 0.05 M $NaBH_4$ solution, obtained by immersion of the Pt electrode into $BiCl_3$/HCl solution under open-circuit conditions for 1 (*a*), 5 (*b*) and 30 (*c*) min. Potential scan rate $v = 50$ mV s^{-1}

used. To facilitate the analysis of the CV curves only anodic going scans for different electrode modification times are presented in Fig. 7a–c. The longer is the immersion time of the Pt electrode into the modifying solution, the more Bi oxy-species-rich catalyst is obtained and the more pronounced shift of wave a1 in the positive potential direction is observed (Fig. 6a, inset). The initial adsorption of BH_4^- ions over the unmodified Pt surface is known to be dissociative and highly favourable at all the potentials of interest (including the open circuit potential) if sufficient free surface sites are available [21]. It requires at least nine Pt surface atoms [21, 72, 20] and produces a high surface coverage of adsorbed hydrogen atoms. The availability of free adsorption sites are changed on the Bi-modified Pt electrode since hydrogen oxidation is entirely inhibited on the Bi-modified Pt electrode when compared to the current response on the unmodified polycrystalline Pt electrode in the background electrolyte (Fig. 3). Bismuth species distinctly change the initial dissociative adsorption step of BH_4^- on Pt by blocking active Pt sites in the borohydride solution and (partially or completely) inhibit surface processes occurring with the respect to wave a1. Hydrogen oxidation, being largely suppressed, could explain the inhibition of borohydride hydrolysis reaction (2) on the Bi-modified Pt electrode.

Scanning the electrode potential to the more positive direction an ill-resolved shoulder at ca. –0.6 V appears for all the different time Bi-modified Pt electrodes (Fig. 7a–c). It develops with the successive potential cycles, simultaneously shifting the onset potential of borohydride oxidation to the negative potential domain, and could be attributed to the oxidation of both borohydride and bismuth oxy-species, similarly to the analogous response for the positive-going potential scan in the supporting electrolyte (Fig. 3). A tremendous increase in borohydride oxidation current occurs giving a current peak in the potential domain of wave a1 from –0.5 to –0.31 V depending on the modification time and scanning cycle applied. The first positive-going scans for borohydride oxidation over the Bi-modified Pt electrodes exhibit about a threefold higher current as compared to that of the unmodified Pt electrode in the mentioned potential region, demonstrating a superior catalytic activity of Bi-modified polycrystalline Pt (Fig. 6a, inset). Thereafter the current drops, passes a dip at ca. –0.05 V and approaches that for the unmodified Pt electrode. The consumption of wave a1 coincides with the peak at ca. –0.1 V for the Bi-modified Pt electrode in a NaOH solution (Fig. 3), which is associated with the enhanced formation of OH_{ad} / oxygenated species on the Pt sites adjacent to Bi adatoms due to lowering the local pzc [73].

A considerable gain of the current on the Bi-modified Pt electrode in the potential domain of wave a1 from –0.5 to –0.31 V could be explained, on the one hand, by gradual conversion of Bi-oxychloride and Bi-hydroxy / oxy species to higher valent Bi-oxygenated surface species in the potential region, associated with initially reversible and weak OH_{ad} adsorption on Pt. At the same time, the massive adsorption of BH_4^- species on the Pt surface was shown to grow sharply beyond ca. –0.4 V by in situ FTIR spectroscopy measurements [20]. Consequently, direct borohydride oxidation by reaction (2) might occur. Moreover, this assumption of borohydride oxidation reaction through a direct reaction pathway could be supported by the number of calculated ca. 8 electrons exchanged per BH_4^- on the PtBi/C catalyst [41].

On the other hand, XPS data (Table 1, Fig. 2) confirmed the presence of both metallic bismuth and its oxy-species on the Pt surface after the spontaneous modification under open-circuit conditions and showed that hydroxylated oxide, assigned as BiO(OH), $Bi(OH)_3$ (Bi_2O_3 in the aqueous media exists under its hydrated form [77] and bismuth oxychloride is predominantly located at the very top of the modifying layer. These data are in line with the XPS data [70], where BiO(OH) and $Bi(OH)_3$ were formed when Bi was in contact with the NaOH solution under open potential conditions. Moreover, when the Bi-modified Pt electrode was exposed to –0.45 V, the presence of Bi_{upd} with specifically adsorbed Bi species on the top of the Bi_{upd} layer was referred [60]. In our case the presence of hydroxylated species on the top of the modifying layer seems to be reasonable and may imply that they act as a donor of hydroxyl species, providing their higher availability for borohydride oxidation. Furthermore, following the potential-pH diagram of bismuth species [77], the domain of wave a1 at ca. –0.245 V coincides with the potential domain of Bi_2O_5 formation. Bi_2O_5 was supposed to serve as active sites for OH_{ad} adsorption in alkaline media [84]. Thus, the changed initial BH_4^- adsorption step and a higher availability of hydroxyl species could aim at the borohydride oxidation reaction through a direct reaction pathway on the Bi-modified polycrystalline Pt electrode and explain the current increase as compared to that of the unmodified Pt surface.

The decreasing part of wave a1 at ca. –0.1 V (Fig. 4) for the Bi-modified Pt electrode, still performing a higher current towards the unmodified Pt electrode, is associated with enhanced formation of OH_{ad} / oxygenated species on the Pt sites adjacent to Bi adatoms (Fig. 3) possibly along with the accumulation of borohydride intermediate species. Concomitantly the presence of these species supposes a decreasing availability of free adjacent Pt atoms, necessary for dissociative adsorption of $BH_{4,ad}$ [45, 72] and points to the different type of dissociative adsorption requiring only 1–3 free Pt atoms [21, 72].

Passing the dip at ca. –0.05 V the borohydride oxidation in the potential domain of wave a2 proceeds on the Pt surface with the strongly adsorbed OH_{ad} or Pt oxides formed, and therefore is less efficient than that on bare platinum [18]. The main oxygen source for borohydride oxidation involves adsorbed OH_{ad} according to the Langmuir-Hinshelwood mechanism [72]. However, the influence of Bi species onto the polarization curve in this potential region remains less significant, and results in a slight current decrease upon cycling, depending on different electrode immersion time into the $BiCl_3$/HCl solution. Possibly the formation of strong surface oxide layers in the presence of irreversibly adsorbed Bi species on polycrystalline Pt [76, 79] along with the accumulated borohydride intermediate species, generated in the case of incomplete dissociation [72], could imply the decrease of the borohydride oxidation process.

Even though, the borohydride oxidation current density over the Bi-modified Pt electrode decreases when successive cycling is applied but finally it achieves some quasi-steady state conditions with the hydrogen oxidation current suppressed implying the inhibition of borohydride hydrolysis reaction (1). Importantly, the integration of the successive positive-going scans starting from the second one results in almost equal overall charges in the potential limit range from –0.9 to 0.8 V (Fig. 7b, inset). They depend on different Pt surface coverages of Bi species developed after various immersion times of the Pt electrode into the modifying solution and are in line with those determined for Pt(111) after different contact times with the Bi-containing solution [85]. A close examination of the electrochemical scanning tunnelling microscopy (EC-STM) coverages during the electrochemical treatments in the mentioned work [85] revealed that after electrochemical reduction the coverages decreased, when compared to those for the open circuit potential (OCP) and did not change after re-oxidation. Nevertheless, the pristine

oxygenated Bi at the OCP and re-oxidised oxygenated Bi were supposed to be chemically identical, however, they differed from the structural point of view. Such structural change during the electrochemical treatments was interpreted by the removal of an oxygen species and a simultaneous shrinkage of the elemental Bi domains during reduction, and the reinsertion of another oxygen species into the compressed domains of Bi along with re-oxidation. Possibly analogous structural changes could take place in our case. On the other hand, almost equal values of the charges obtained by us might be indicative of the development of a relatively stable Bi-oxyspecies adlayer on the polycrystalline Pt electrode surface during multifold cycling, nevertheless, at different potentials different forms of Bi-species dominate and undergo transformation in valency. Anyway a comparatively high electrocatalytic activity of a newly prepared Bi-modified Pt catalyst made by irreversible adsorption of Bi-species in a hydrochloric acid solution gives grounds for further development of more stable and durable catalysts that could be applied for modification of realistic titanium, carbon or graphene supported Pt nanoparticle catalysts relevant to borohydride fuel cell anode operation.

CONCLUSIONS

The spontaneous modification of the polycrystalline Pt surface by immersion of the Pt electrode into the $BiCl_3$/HCl solution under open-circuit conditions for 1 or 30 min indicates the presence of both metallic bismuth and its oxy-species on the Pt surface with bismuth oxychloride / (hydr)oxide predominantly located at the very top of the modifying layer. The Bi oxyspecies-rich catalyst was obtained in the case of Pt electrode modification for 30 min. It has been determined that borohydride oxidation over the Bi-modified polycrystalline Pt electrode obtained by irreversible adsorption of Bi species, regardless of the different electrode immersion times into a $BiCl_3$/HCl solution, results in a largely suppressed hydrogen oxidation implying the inhibition of borohydride hydrolysis reaction (1) and shows a higher catalytic activity for borohydride oxidation in the further potential domain associated with initially reversible and weak OH_{ad} adsorption on Pt. A considerable gain in the current on the Bi-modified polycrystalline Pt electrode in the potential region of wave a1 could be explained, on the one hand, by a gradual conversion of Bi-oxychloride and Bi-hydroxy / oxy surface species to higher valent Bi-oxygenated surface species. On the other hand, the presence of hydroxylated species on the top of the modifying layer may imply that they act as a donor of hydroxyl species, providing their higher availability on the Bi-modified polycrystalline Pt surface for borohydride oxidation. Evidently, changed initial BH_4^- ion adsorption step in the presence of irreversibly adsorbed Bi species and a higher availability of hydroxyl species on the Bi-modified Pt electrode could aim at borohydride oxidation reaction through a direct reaction pathway. The electrocatalytic activity of a newly prepared Bi-modified Pt catalyst made by irreversible adsorption of Bi-species in hydrochloric acid gives grounds for further development of the former catalysts with improved features that could be, in turn, adopted for modification of variety realistic titanium, carbon or graphene supported Pt nanoparticle catalysts relevant to borohydride fuel cell anode operation. A concerted experimental and theoretical effort is much required in advancing the application of the borohydride fuel cell. Future investigations focused on fundamental understanding of this complex, multi-step, up to eight-electron transfer of the BH_4^- electrooxidation process on the Bi-modified Pt surface are underway.

Received 27 May 2014
Accepted 17 June 2014

References

1. D. M. F. Santos, C. A. C. Sequeira, *Renew. Sust. Energ. Rev*., **15**, 3980 (2011).
2. J.-H. Wee, *J. Power Sources*, **155**, 329 (2006).
3. C. Ponce de Leon, F. C. Walsh, D. Pletcher, D. J. Browning, J. B. Lakeman, *J. Power Sources*, **155**, 172 (2006).
4. B. H. Liu, Z. P. Li, S. Suda, *J. Power Sources*, **187**, 527 (2009).
5. B. H. Liu, Z. P. Li, S. Suda, *J. Power Sources*, **187**, 291 (2009).
6. J. Ma, N. A. Choudhury, Y. Sahai, *Renew. Sust. Energ. Rev*., **14**, 183 (2010).
7. H. Wee, *J. Power Sources*, **161**, 1 (2006).
8. R. L. Pecsok, *J. Am. Chem. Soc*., **75**, 2862 (1953).
9. J. H. Morris, H. J. Gysling, D. Reed, *Chem. Rev*., **85**, 51(1985).
10. S. Amendola, *J. Powers Sources*, **84**, 130 (1999).
11. B. H. Liu, Z. P. Li, S. Suda, *Electrochim. Acta*, **49**, 3097 (2004).
12. E. Gyenge, M. Atwan, D. Northwood, *J. Electrochem. Soc*, **153**, A150 (2006).
13. L. C. Nagle, J. F. Rohan, *J. Electrochem. Soc*., **153**, C773 (2006).
14. M. E. Indig, R. N. Snyder, *J. Electrochem. Soc*., **109**, 1104 (1962).
15. M. V. Mirkin, H. Yang, A. J. Bard, *J. Electrochem. Soc.,* **139**, 2212 (1992).
16. J. P. Elder, A. Hickling, *Trans. Faraday Soc*., **58**, 1852 (1962).
17. M. Chatenet, F. Micoud, I. Roche, E. Chainet, *Electrochim. Acta*, **51**, 5459 (2006).
18. D. A. Finkelstein, N. D. Mota, J. L. Cohen, H. D. Abruña, *J. Phys. Chem. C*, **113**, 19700 (2009).
19. M. Chatenet, F. H. B. Lima, E. A. Ticianelli, *J. Electrochem. Soc*., **157**, B697 (2010).
20. B. M. Concha, M. Chatenet, E. A. Ticianelli, F. H. B. Lima, *J. Phys. Chem. C*, **115**, 12439 (2011).
21. G. Rostamikia, M. J. Janik, *Electrochim. Acta*, **55**, 1175 (2010).
22. M. C. S. Escaño, E. Gyenge, R. L. Arevalo, H. Kasai, *Journal Phys. Chem. C.*, **115**, 19883 (2011).
23. G. Rostamikia, M. J. Janik, *Electrochem. Soc*., **156**, B86 (2009).

24. C. Celik, F. G. Boyanci San, H. I. Sarac, *J. Power Sources,* **185**, 197 (2008).
25. M. H. Atwan, C. L. B. Macdonald, D. O. Northwood, E. L. Gyenge, *J. Power Sources*, **158**, 36 (2006).
26. E. Gyenge, *Electrochim. Acta*, **49**, 965 (2004).
27. M. H. Atwan, D. O. Northwood, E. L. Gyenge, *Int. J. Hydrogen Energ.*, **32**, 3116 (2007).
28. P. Krishnan, T.-H. Yang, S. G. Advani, A. K. Prasad, *J. Power Sources*, **182**, 106 (2008).
29. F. H. B. Lima, A. M. Pasqualeti, M. B. Molina Concha, M. Chatenet, E. A. Ticianelli, *Electrochim. Acta*, **84**, 202 (2012).
30. B. Molina Concha, M. Chatenet, C. Coutanceau, F. Hahn, *Electrochem. Comm.*, **11**, 223 (2009).
31. B. Molina Concha, M. Chatenet, F. Mailard, E. A. Ticianelli, F. H. B. Lima, *J. Phys. Chem.*, **12**, 11509 (2010).
32. B. H. Liu, Z. P. Li, S. Suda, *J. Electrochem. Soc.*, **150**, A398 (2003).
33. Z. P. Li, B. H. Liu, J. K. Zhu, S. Suda, *J. Power Sources*, **163**, 555 (2006).
34. H. Dong, R. X. Feng, X. P. Ai, Y. L. Cao, H. X. Yang, C. S. Cha, *J. Phys. Chem. B.*, **109**, 10896 (2005).
35. K. Wang, J. Lu, L. Zhuang, *J. Phys. Chem. C*, **111**, 7456 (2007).
36. E. Gyenge, M. Atwan, D. Northwood, *J. Electrochem. Soc.*, **153**, A150 (2006).
37. H. Cheng, K. Scott, *J. Appl. Electrochem.*, **36**, 1361 (2006).
38. M. H. Atwan, D. O. Northwood, E. L. Gyenge, *Int. J. Hydrogen Energ.*, **30**, 1323 (2005).
39. H. Cheng, K. Scott, *Electrochim. Acta*, **51**, 3429 (2006).
40. D. Miliauskas, R. Tarozaitė, L. T. Tamašiūnaitė, *Mater. Sci. (Medžiagotyra)*, **14**, 20 (2008).
41. M. Simões, S. Baranton, C. Countanceau, *Electrochim. Acta*, **56,** 580 (2010).
42. V. W. S. Lam, E. L. Gyenge, *J. Electrochem. Soc.,* **155**, B1155 (2008).
43. B. Molina Concha, M. Chatenet, *Electrochim. Acta*, **54**, 6130 (2009).
44. I. Martins, M. C. Nunes, R. Koch, L. Martins, M. Bazzaqui, *Electrochim. Acta*, **52**, 6443 (2007).
45. S. P. E. Smith, H. D. Abruña, *J. Electroanal. Chem.*, **467**, 4349 (1999).
46. S. P. E. Smith, K. F. Ben-Dor, H. D. Abruña, *Langmuir*, **15**, 7325 (1999).
47. S. P. E. Smith, K. F. Ben-Dor, H. D. Abruña, *Langmuir*, **16**, 787 (2000).
48. J. Clavilier, A. Fernandez-Vega, J. M. Feliu, A. Aldaz, *J. Electroanal. Chem.*, **261**, 113 (1989).
49. J. Clavilier, A. Fernandez-Vega, J. M. Feliu, A. Aldaz, *J. Electroanal. Chem.*, **258**, 89 (1989).
50. I. G. Casella, M. Gatta, M. Contursi, *J. Electroanal. Chem.*, **561**, 103 (2004).
51. R. R. Adžic, in: H. Gerisher, C. W. Tobias (eds.), *Advances in Electrochemistry and Electrochemical Engineering*, p. 159, Wiley, NewYork (1984).
52. S. Szabo, F. Nagy, *J. Electroanal. Chem.*, **87**, 261 (1978).
53. J. Clavilier, J. M. Feliu, A. Aldaz, *J Electroanal. Chem.*, **243**, 419 (1988).
54. S. A. Campbell, R. Parsons, *J. Chem. Soc. Faraday Trans.*, **88**, 833 (1992).
55. J. Solla-Gullón, P. Rodríguez, E. Herrero, A. Aldaz, J. M. Feliu, *Phys. Chem. Chem. Phys.*, **10**, 1349 (2008).
56. P. Rodríguez, E. Herrero, J. Solla-Gullón, F. J. Vidal-Iglesias, A. Aldaz, J. M. Feliu, *Electrochim. Act*a, **50**, 4308 (2005).
57. V. Pautienė, L. Tamašiūnaitė-Tamašauskaitė, A. Sudavičius, G. Stalnionis, Z. Jusys, *J. Solid State Electrochem.*, **14**, 1675 (2010).
58. D. Briggs, M. P. Seah, *Practical Surface Analysis*, 2nd ed., Vol. 1, John Wiley and Sons, New York (1993).
59. U. W. Hamm, D. Kramer, R. S. Zhai, D. M. Kolb, *Electrochim. Acta*, **43**, 2969 (1998).
60. G. Wittstok, A. Strübing, R. Szargan, G. Werner, *J. Electroanal. Chem.*, **444**, 61 (1998).
61. A. V. Tripković, K. D. J. Popović, R. M. Stevanović, R. Socha, A. Kowal, *Electrochem. Comm.*, **8**, 1492 (2006).
62. X. Chang, J. Huang, C. Cheng, W. Sha, X. Li, G. Ji, *J. Hazard. Mater.*, **173**, 765 (2010).
63. C. Wang, C. Shao, Y. Liu, L. Zhang, *Scripta Materialia*, **59**, 332 (2008).
64. D. R. Blasini, D. Rochefort, E. Fachini, L. R. Aldena, F. J. DiSalvo, C. R. Cabrera, H. D. Abruña, *Surf. Sci.*, **600**, 2670 (2006).
65. X. Yu, P. G. Pickup, *Electrochim. Acta*, **56**, 4037 (2011).
66. B. V. Tilak, B. E. Conway, H. Angerstain-Kozlowska, *J. Electroanal. Chem.*, **48**, 1 (1973).
67. D. M. Dražić, A. V. Tripković, K. D. Popović, D. J. Lović, *J. Electroanal. Chem.*, **466**, 155 (1999).
68. N. M. Marković, T. J. Schmidt, B. N. Grgur, H. A. Gasteiger, P. N. Ross, Jr. R. J. Behm, *J. Phys. Chem. B.*, **103**, 8568 (1999).
69. A. V. Tripković, K. D. J. Popović, D. J. Lović, *Electrochim. Acta*, **46**, 3163 (2001).
70. N. M. Marković, H. A. Gasteiger, P. N. Ross, *J. Phys. Chem. B*, **100**, 6715 (1996).
71. N. M. Marković, S. T. Sarraf, H. A. Gasteiger, P. N. Ross, *J. Chem. Soc., Faraday Trans.*, **92**, 3719 (1996).
72. V. W. S. Lam, D. C. W. Kannangara, A. Alfantazi, E. L. Gyenge, *J. Phys. Chem. C.*, **115**, 2727 (2011).
73. T. J. Schmidt, P. N. Ross, N. M. Marković, *J. Phys. Chem. B*, **105**, 12082 (2001).
74. S. P. E. Smith, H. D. Abruña, *J. Phys. Chem. B*, **102**, 3506 (1998).
75. B. J. Bowles, *Electrochim. Acta*, **15**, 737 (1970).
76. T. J. Schmidt, V. Stamenković, G. A. Attard, N. M. Marković, P. N. Jr Ross., *Langmuir*, **17**, 7613 (2001).
77. J. Van Muylder, M. Pourbaix, *Atlas d' équilibres électrochimiques à 25 °C*, Gauthier-Villars & Cie, Paris (1963).
78. F. Kadirgan, B. Beden, F. C. Lamy, *J. Electroanal. Chem.*, **143**, 135 (1983).
79. R. R. Adžic, N. M. Marković, *Electrochim. Acta*, **30**, 1473 (1985).
80. H. Angerstain-Kozlowska, B. E. Conway, W. B. A. Sharp, *J. Electroanal. Chem.*, **43**, 9 (1973).
81. L. Demarconnay, C. Countanceau, J.-M. Léger, *Electrochim. Acta*, **53**, 3232 (2008).
82. B. Beden, F. Kadirgan, C. Lamy, J.-M. Léger, *J. Electroanal. Chem.*, **142**, 171 (1982).

83. B. Molina Concha, M. Chatenet, *Electrochim. Acta*, **54**, 6119 (2009).
84. M. Yang, *J. Power Sources*, **229**, 42 (2013).
85. J. Kim, C. K. Rhee, *J. Solid State Electrochem.*, **17**, 3109 (2013).

Dijana Šimkūnaitė, Loreta Tamašauskaitė-Tamašiūnaitė, Vitalija Jasulaitienė, Algirdas Selskis

BOROHIDRIDO ELEKTROOKSIDACIJA ANT Bi JUNGINIAIS MODIFIKUOTOS POLIKRISTALINĖS PLATINOS ELEKTRODO

S a n t r a u k a

Tirta borohidrido oksidacija ant Bi junginiais modifikuotos Pt elektrodo šarminiuose tirpaluose, turinčiuose 0,05 M $NaBH_4$ ir 1 M NaOH, panaudojant paviršiaus analizės (XPS ir SEM) ir elektrocheminius (ciklinės voltametrijos) metodus. XP spektroskopijos duomenų analizė parodė, kad atviros grandinės sąlygomis skirtingą laiką išlaikius Pt elektrodą $BiCl_3$, ištirpinto koncentruotos rūgšties modifikavimo tirpale ant Pt paviršiaus, yra tiek metalinis Bi, tiek Bi-oksi/hidroksi/oksido junginiai. Šiais junginiais modifikuotas Pt elektrodas pasižymėjo geresnėmis elektrokatalitinėmis savybėmis, palyginti su nemodifikuotos Pt elektrodu, stipriai slopino vandenilio oksidaciją, o kartu ir borohidrido hidrolizės reakciją. Žymus srovės padidėjimas ant Bi junginiais modifikuotos Pt elektrodo, tikėtina, yra susijęs su laipsniška Bi-oksichlorido ir Bi-hidroksi/oksi paviršiaus junginių transformacija į aukštesnio valentingumo deguonį turinčius Bi junginius, kartu vykstant borohidrido oksidacijai. Manoma, kad hidroksilą turintys Bi junginiai, lokalizavęsi modifikuojančio sluoksnio paviršiuje, gali būti laikomi OH grupės donorais, suteikiančiais daugiau hidroksilo junginių ant Bi-modifikuotos Pt paviršiaus, reikalingų borohidrido oksidacijai.